



A LETTERS JOURNAL EXPLORING
THE FRONTIERS OF PHYSICS

OFFPRINT

High-precision simulation of the height distribution for the KPZ equation

ALEXANDER K. HARTMANN, PIERRE LE DOUSSAL, SATYA N.
MAJUMDAR, ALBERTO ROSSO and GREGORY SCHEHR

EPL, **121** (2018) 67004

Please visit the website
www.epljournal.org

Note that the author(s) has the following rights:

- immediately after publication, to use all or part of the article without revision or modification, **including the EPLA-formatted version**, for personal compilations and use only;
- no sooner than 12 months from the date of first publication, to include the accepted manuscript (all or part), **but not the EPLA-formatted version**, on institute repositories or third-party websites provided a link to the online EPL abstract or EPL homepage is included.

For complete copyright details see: <https://authors.eplletters.net/documents/copyright.pdf>.



epl

A LETTERS JOURNAL EXPLORING
THE FRONTIERS OF PHYSICS

AN INVITATION TO SUBMIT YOUR WORK

epljournal.org

The Editorial Board invites you to submit your letters to EPL

EPL is a leading international journal publishing original, innovative Letters in all areas of physics, ranging from condensed matter topics and interdisciplinary research to astrophysics, geophysics, plasma and fusion sciences, including those with application potential.

The high profile of the journal combined with the excellent scientific quality of the articles ensures that EPL is an essential resource for its worldwide audience. EPL offers authors global visibility and a great opportunity to share their work with others across the whole of the physics community.

Run by active scientists, for scientists

EPL is reviewed by scientists for scientists, to serve and support the international scientific community. The Editorial Board is a team of active research scientists with an expert understanding of the needs of both authors and researchers.



epljournal.org

OVER

568,000

full text downloads in 2015

18 DAYS

average accept to online
publication in 2015

20,300

citations in 2015

*"We greatly appreciate
the efficient, professional
and rapid processing of
our paper by your team."*

Cong Lin
Shanghai University

Six good reasons to publish with EPL

We want to work with you to gain recognition for your research through worldwide visibility and high citations. As an EPL author, you will benefit from:

- 1 Quality** – The 60+ Co-editors, who are experts in their field, oversee the entire peer-review process, from selection of the referees to making all final acceptance decisions.
- 2 Convenience** – Easy to access compilations of recent articles in specific narrow fields available on the website.
- 3 Speed of processing** – We aim to provide you with a quick and efficient service; the median time from submission to online publication is under 100 days.
- 4 High visibility** – Strong promotion and visibility through material available at over 300 events annually, distributed via e-mail, and targeted mailshot newsletters.
- 5 International reach** – Over 3200 institutions have access to EPL, enabling your work to be read by your peers in 100 countries.
- 6 Open access** – Articles are offered open access for a one-off author payment; green open access on all others with a 12-month embargo.

Details on preparing, submitting and tracking the progress of your manuscript from submission to acceptance are available on the EPL submission website epletters.net.

If you would like further information about our author service or EPL in general, please visit epijournal.org or e-mail us at info@epijournal.org.

EPL is published in partnership with:



European Physical Society



Società Italiana
di Fisica

edp sciences **IOP Publishing**

EDP Sciences

IOP Publishing

High-precision simulation of the height distribution for the KPZ equation

ALEXANDER K. HARTMANN^{1,2}, PIERRE LE DOUSSAL³, SATYA N. MAJUMDAR¹, ALBERTO ROSSO¹
and GREGORY SCHEHR²

¹ *Institut für Physik, Universität Oldenburg - 26111 Oldenburg, Germany*

² *LPTMS, CNRS, Univ. Paris-Sud, Université Paris-Saclay - 91405 Orsay, France*

³ *CNRS-Laboratoire de Physique Théorique de l'Ecole Normale Supérieure - 24 rue Lhomond, 75231 Paris Cedex, France*

received 7 February 2018; accepted in final form 20 April 2018
published online 18 May 2018

PACS 75.10.Nr – Spin-glass and other random models
PACS 05.10.Ln – Monte Carlo methods
PACS 05.20.-y – Classical statistical mechanics

Abstract – The one-point distribution of the height for the continuum Kardar-Parisi-Zhang (KPZ) equation is determined numerically using the mapping to the directed polymer in a random potential at high temperature. Using an importance sampling approach, the distribution is obtained over a large range of values, down to a probability density as small as 10^{-1000} in the tails. Both short and long times are investigated and compared with recent analytical predictions for the large-deviation forms of the probability of rare fluctuations. At short times the agreement with the analytical expression is spectacular. We observe that the far left and right tails, with exponents $5/2$ and $3/2$, respectively, are preserved also in the region of long times. We present some evidence for the predicted non-trivial crossover in the left tail from the $5/2$ tail exponent to the cubic tail of the Tracy-Widom distribution, although the details of the full scaling form remain beyond reach.

Copyright © EPLA, 2018

Introduction. – The (1+1)-dimensional Kardar-Parisi-Zhang (KPZ) equation describes the non-linear stochastic growth of an interface [1]. It is also relevant in a wide variety of physical models ranging from directed polymers in random media [1–7] to asymmetric exclusion process models for the transport of interacting particles [8–11] and has a number of experimental realisations [12–14]. The interface is described by a field $h(x, t)$ that denotes its height at the position x and at time t . The KPZ equation of motion is

$$\partial_t h = \nu \partial_x^2 h + \frac{\lambda_0}{2} (\partial_x h)^2 + \sqrt{D} \xi(x, t), \quad (1)$$

where $\nu > 0$ gives the strength of the diffusive relaxation, $\lambda_0 > 0$ is the coefficient of the non-linearity and $\xi(x, t)$ is a Gaussian white noise with zero mean and $\langle \xi(x, t) \xi(x', t') \rangle = \delta(x - x') \delta(t - t')$. From dimensional analysis it is natural to introduce the following characteristic scales of space $x^* = (2\nu)^3 / (D\lambda_0^2)$, time $t^* = 2(2\nu)^5 / (D^2\lambda_0^4)$ and height $h^* = \frac{2\nu}{\lambda_0}$. For simplicity in the following we will work in rescaled units: $x/x^* \rightarrow x$,

$t/t^* \rightarrow t$, $h/h^* \rightarrow h$. At large times $t \gg 1$ it is known that, due to the non-linearity, the interface moves with a finite deterministic velocity v_∞ which depends on the initial condition.

In the last decades tremendous progress has been achieved in obtaining exact results on the statistics of the height fluctuations [2,15–17], *e.g.*, of the centred height at one space point defined as $H(t) = h(x=0, t) - v_\infty t + \frac{1}{2} \ln t$. This centring takes into account the solution in the case of absence of noise, see eq. (9) in ref. [18]. In particular the best studied case corresponds to a narrow wedge initial condition $h(x, t=0) = -|x|/\delta$ with $\delta \ll 1$ which gives rise at late times to the experimentally relevant curved or *droplet* profile. In this case the fluctuations of H can be expressed, for any time t , in terms of a Fredholm determinant [6,7,19,20]. Despite this exact result, since the Fredholm determinant is a complicated mathematical object, it remains very challenging to obtain useful explicit information about the statistics of H at a given time t . It is known that at short time, $t \ll 1$, the non-linear term in eq. (1) is less important compared to the linear Laplacian

term. In this limit the typical fluctuations of H are well described by the Edwards-Wilkinson equation (*i.e.*, eq. (1) with $\lambda_0 = 0$). Hence in the short-time limit the typical fluctuations of H are of order $\sim t^{1/4}$ and Gaussian. On the other hand, at large time, $t \gg 1$, the typical fluctuations of order $\sim t^{1/3}$ are described by the Tracy-Widom (TW) distribution associated to the typical fluctuations of the largest eigenvalue of random matrices belonging to the Gaussian Unitary Ensemble (GUE) [21]. The TW distribution has been observed experimentally in nematic liquid crystals which exhibit KPZ growth laws [12,13]. More recently there has been an increasing interest in computing the probability of rare fluctuations of H away from its typical values. The general problem of large deviations in non-equilibrium situations is connected to the question of defining the proper free energy and entropy functionals for these systems, see refs. [22–24]. This large-deviation problem can be addressed both for short and large times. The question of whether and how the tails evolve with time is important for many models in the KPZ class. Here we explore this issue numerically for the KPZ equation itself, and compare with recent analytical predictions. In particular, thanks to a short-time expansion of the exact Fredholm determinant formula, an explicit form for the short-time distribution $P(H, t)$, with $t \ll 1$, has been obtained [18]. It takes a large-deviation form:

$$P(H, t) \sim c(t) e^{-\frac{1}{\sqrt{t}} \phi_{\text{short}}(H)}, \quad (2)$$

where $c(t)$ is a time-dependent normalisation constant. The exact form of $\phi_{\text{short}}(H)$ is given in [18], its asymptotic behaviour, which can also be obtained using weak noise theory [25], reads [18,25]

$$\phi_{\text{short}}(H) \simeq \begin{cases} \frac{4}{15\pi} |H|^{5/2}, & H \rightarrow -\infty, \\ \frac{H^2}{\sqrt{2\pi}}, & |H| \ll 1, \\ \frac{4}{3} H^{3/2}, & H \rightarrow +\infty. \end{cases} \quad (3)$$

As expected, the typical fluctuations around $H = 0$ are Gaussian, but the tails are asymmetric. In particular the right tail, $H \rightarrow +\infty$, coincides exactly with the TW tail, while the left tail is characterised by a different $\frac{4}{15\pi} |H|^{5/2}$ behaviour, different from the $\frac{1}{12} |H|^3$ of the TW distribution. The tail behaviours $\propto |H|^{5/2}$ (left) and $\propto H^{3/2}$ (right) seem to be quite robust with respect to different initial conditions: indeed this has been obtained in the regime of short times also for flat as well as for stationary initial conditions albeit with different prefactors [25–28]. In addition the central part of the distribution depends on the initial condition.

Exact results for the large deviations have also been obtained in the regime of long times, $t \gg 1$, for the droplet initial condition. In particular $P(H, t)$ displays

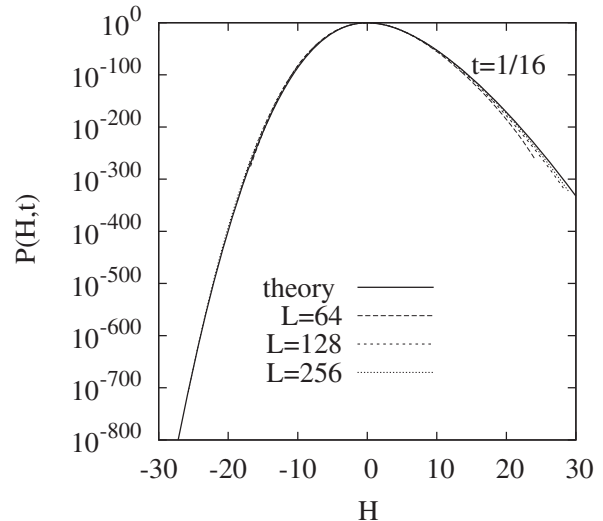


Fig. 1: Distribution of $P(H, t)$ for a short time $t = 1/16$ for three different lengths $L = 64$, $L = 128$ and $L = 256$. The solid line indicates the analytical result in eq. (2) obtained in ref. [18]. The agreement between numerical and analytical results is extremely good (on the left tail, down to values of the order 10^{-800}).

three different regimes [29]:

$$P(H, t) \sim \begin{cases} e^{-t^2 \Phi_-(H/t)}, & H \sim \mathcal{O}(t) < 0, \\ \frac{1}{t^{1/3}} f_2 \left[\frac{H}{t^{1/3}} \right], & H \sim \mathcal{O}(t^{1/3}), \\ e^{-t \Phi_+(H/t)}, & H \sim \mathcal{O}(t) > 0, \end{cases} \quad (4)$$

where $f_2(z)$ is the GUE TW distribution. The tails have also been computed explicitly. The right tail rate function [29]

$$\Phi_+(z) = \frac{4}{3} z^{3/2} \quad (5)$$

coincides exactly with the TW tail as already observed in the short-time regime. The left tail rate function was predicted in [30] to be

$$\Phi_-(z) = \frac{4}{15\pi^6} (1 - \pi^2 z)^{5/2} - \frac{4}{15\pi^6} + \frac{2}{3\pi^4} z - \frac{1}{2\pi^2} z^2. \quad (6)$$

Note that eq. (6) exhibits a crossover between two distinct tail behaviours of $P(H, t)$ for large negative H : when $z = \frac{H}{t} \rightarrow 0$ one has $\Phi_-(z) \simeq |z|^3/12$ such that from the first line of eq. (4) one recovers the left tail of the TW distribution, *i.e.*, $P(H, t) \sim e^{-|H|^3/(12t)}$. On the other hand, when $z = \frac{H}{t} \rightarrow -\infty$ one has $\Phi_-(z) \simeq \frac{4}{15\pi} |z|^{5/2}$, which coincides with the left tail of the short-time large deviation given in the first line of eq. (3), *i.e.*, $P(H, t) \sim e^{-\frac{4}{15\pi} |H|^{5/2}/\sqrt{t}}$. The results for the left tail were rigorously confirmed by a different approach [31], which is based on a correspondence of the KPZ equation to the Airy point process.

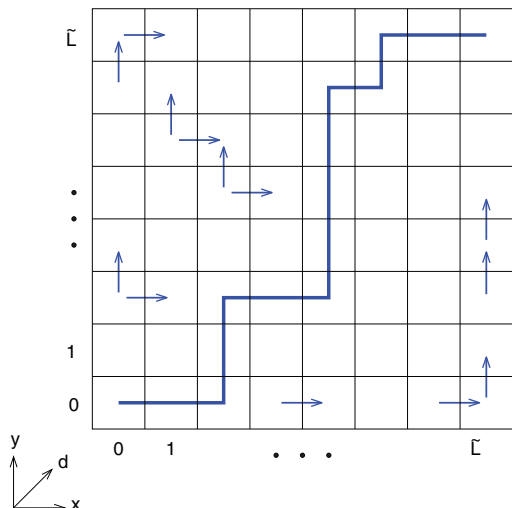


Fig. 2: (Colour online) Setup of the lattice with examples of possible bonds of the polymer (small arrows) and one example of a polymer (thick line). All polymers start at $(0, 0)$ and end in (\tilde{L}, \tilde{L}) and, therefore, consist of $L = 2\tilde{L}$ bonds.

For intermediate time, $t \sim 1$, only the cumbersome Fredholm determinant formula is available and no explicit information is known for large fluctuations of H . Indeed numerical results focused only on the typical fluctuations [6,18] as the study of the tails requires a huge number of samples.

In this paper we use importance sampling techniques and study numerically the full large deviations of H both for short and intermediate time. This allows us to explore the tail statistics with an unprecedented precision of the order of 10^{-1000} . In the short-time regime our results perfectly agree with the theoretical prediction in eq. (3) (see fig. 1) and the asymptotic behaviour of the tails is clearly seen in fig. 3, both for the left tail (top panel) and the right tail (bottom panel). For the intermediate times our results are consistent with the following scenario (see fig. 4); i) the right tail $P(H, t) \sim \exp(-\frac{4}{3}H^{3/2}/\sqrt{t})$ remains valid at all times; ii) the left tail is well described by $\Phi_-(z)$ for large negative $z = H/t$, *i.e.*, the $5/2$ exponent remains valid at all times; iii) the small z behaviour of $\Phi_-(z)$ and the typical fluctuations of H have not reached yet the TW limiting behaviour. Larger times than the ones accessible in our simulations are needed to observe the large time TW behaviour and to fully confirm the form (6) for $\Phi_-(z)$.

Model and algorithm. – There is a standard mapping between the height in the KPZ and the free energy of a directed polymer at high temperature embedded in a 1+1 random potential [6,32]. For a polymer of size $L = 2\tilde{L}$ bonds, the realisation of the disordered potential is given by a two-dimensional lattice of $(\tilde{L} + 1) \times (\tilde{L} + 1)$ random numbers $V[x][y]$ ($x, y = 0, 1, \dots, \tilde{L}$) drawn from a Gaussian distribution $N(0, 1)$, *i.e.*, with mean 0 and variance 1. We consider all polymers which start at $(0, 0)$ and end at (\tilde{L}, \tilde{L}) , such that the polymer continues onto

neighbouring sites of the lattice given that the “diagonal” direction $d = x + y$ increases by one. The geometric setup is shown in fig. 2.

A polymer visiting a set P of sites has an energy

$$E_V(P) = \sum_{(x,y) \in P} V[x][y]. \quad (7)$$

We are interested in the canonical ensemble, where each polymer in the disorder landscape $V \equiv \{V[x][y]\}$ is connected to a heat bath with temperature T and exhibits a Boltzmann weight

$$w_V(P) = e^{-E_V(P)/T}. \quad (8)$$

Therefore, for a given disorder realisation V the partition function $Z(V)$ is given by

$$Z(V) = \sum_P w_V(P), \quad (9)$$

where the sum runs over all possible polymers with requirements as explained above. Due to the requirement that the polymer extends only in increasing diagonal value d , the partition function can be calculated recursively using

$$Z[x][y] = (Z[x-1][y] + Z[x][y-1])e^{-V[x][y]/T}, \quad (10)$$

where $Z[x][y]$ is the partition function of the polymer starting at $(0, 0)$ and ending at (x, y) . Thus, the partition function defined in eq. (9) is given by $Z(V) = Z[\tilde{L}][\tilde{L}]$ and requires $O(\tilde{L}^2)$ steps to be computed. The mapping between the free energy of the directed polymer at temperature T and the KPZ height at time t reads

$$H = \log(Z(V)/\bar{Z}), \quad (11)$$

$$t = \frac{2L}{T^4}, \quad (12)$$

where \bar{Z} is the disorder average partition function. We are interested in the distribution $P(H, t)$ over the disorder.

The importance sampling algorithm. In principle one could obtain an estimate of $P(H, t)$ numerically from *direct sampling*: One generates many disorder realisations (say $\sim 10^6$). For each realisation $Z(V)$ is computed. Then \bar{Z} is estimated by averaging over all samples, and the distribution is the histogram of the values of H according to eq. (11). Nevertheless, this limits the smallest probabilities which can be resolved, *e.g.*, 10^{-6} .

Therefore, we follow here a different approach. To estimate $P(H, t)$ for a much larger range, where probabilities (or corresponding densities) smaller than, *e.g.*, 10^{-1000} may appear, we will use a more powerful approach, called *importance sampling* as discussed in refs. [33,34]. This approach has been successfully applied in many cases to obtain the tails of distributions arising in equilibrium and non-equilibrium situations, *e.g.*, the number of components of Erdős-Rényi (ER) random graphs [35], the partition function of Potts models [36], ground-state energies of

directed polymers in random media [37], the distribution of free energies of RNA secondary structures [38], some large-deviation properties of random matrices [39,40], the distribution of endpoints of fractional Brownian motion with absorbing boundaries [41], the distribution of work performed by an Ising system [42], or the distributions of area and perimeter of random convex hulls [43,44].

To keep the paper self-contained we now briefly outline the method. Note that the approach has already been applied, in a slight variant, to directed polymers in disordered media, at zero temperature [37]. The basic idea is to sample the different disorder realisations V with an additional exponential bias $\exp(-H(V)/\theta)$ with θ as adjustable parameter. Note that if $\theta > 0$ the configurations with a negative H become more likely, conversely for $\theta < 0$ the configurations with a positive H are favoured. A standard Markov-chain Monte Carlo simulation is then used to sample the biased configurations [45,46]. At each time step a new disorder realisation V^* is proposed by replacing on the current realisation V a certain fraction r of the random numbers $V[x][y]$ by new Gaussian numbers. The new disorder realisation is then accepted with the Metropolis-Hastings probability

$$p_{\text{Met}} = \min\{1, e^{-[H(V^*)-H(V)]/\theta}\}, \quad (13)$$

otherwise the old configuration is kept [47]. Note that the average partition function \bar{Z} appearing in the definition of H (11) drops out of the Metropolis probability, *i.e.*, it is not needed here. By construction, the algorithm fulfils detailed balance. Clearly the algorithm is also ergodic, since within a sufficient number of steps, each possible realisation may be constructed. Thus, in the limit of infinitely long Markov chains, the distribution of biased disorder realisations will follow the probability

$$q_\theta(V) = \frac{1}{Q(\theta)} P_{\text{dis}}(V) e^{-H(V)/\theta}, \quad (14)$$

where $P_{\text{dis}}(V)$ is the original disorder distribution (here a simple product of independent Gaussians) and $Q(\theta) = \sum_V P_{\text{dis}}(V) e^{-H(V)/\theta}$ is the normalisation factor. Note that $Q(\theta)$ also depends on L and T , which we omit here in the notation for brevity. $Q(\theta)$ is generally unknown but can be determined, see below. Thus, the output of this Markov chain allows to construct a biased histogram $P_\theta(H, t)$. In order to get the correct histogram $P(H, t)$ one should re-weight the obtained result:

$$P(H, t) = e^{H/\theta} Q(\theta) P_\theta(H). \quad (15)$$

Hence, the target distribution $P(H, t)$ can be estimated, up to a normalisation constant $Q(\theta)$. For each value of the parameter θ , a specific range of the distribution $P(H, t)$ will be sampled: using a positive (respectively, negative) parameter allows to sample the region of a distribution at the left (respectively, at the right) of its peak.

Technical details. To sample a wide range of values of H , one chooses a suitable set of parameters $\{\theta_{-N_n}, \theta_{-N_n+1}, \dots, \theta_{N_p-1}, \theta_{N_p}\}$, N_n and N_p being the number of negative and positive parameters, to access the large deviation regimes (left and right). The normalisation constants $Q(\theta)$ are obtained by first computing the histogram using direct sampling, which is well normalised and corresponds to $\theta = \infty$. Then, for θ_{+1} , one matches the right part of the biased histogram with the left tail of the unbiased one and for θ_{-1} , one matches the left part of the biased histogram with the right tail of the unbiased one. Similarly one iterates for the other values of θ and the corresponding *relative* normalisation constants can be obtained.

The main drawback of our method is that as for any Markov-chain Monte Carlo simulation, it has to be equilibrated and this may take a large number of steps. To speed the simulation up, *parallel tempering* was used [48]. Here, a parallel implementation using the *Message Passing Interface (MPI)* was applied, such that each computing core was responsible in parallel for an independent realisation $V_i(s)$ at a given θ_i . After 1000 Monte Carlo steps, one parallel-tempering sweep was performed and the parameters θ_i and θ_{i+1} were exchanged between two computing cores. The parameter r is fixed with the criterion that the empirical acceptance rate of the parallel-tempering exchange step is about 0.5 for all pairs of neighbouring θ_i . A pedagogical explanation and examples of this sampling procedure can be found in ref. [49].

Results. – We have performed extensive numerical simulations [50] for polymer lengths $L = 64, 128$ and 256 and considered three different times corresponding to short times $t \ll 1$ ($t = 1/16, 1/4$) and (quite) large times ($t = 32$). In the numerical simulations the temperatures T were chosen according to eq. (12).

For each set of values L and T , the numbers N_n and N_p and the values of parameters $\{\theta_{-N_n}, \dots, \theta_{N_p}\}$ were determined from numerical experiments. For small sizes $L = 64$ the number $N_n + N_p$ of parameters was typically about 30 with values, *e.g.*, $\theta \in [-0.5, -0.015] \cup [0.06, 0.5]$. For the largest size $L = 256$ up to $N_n + N_p = 117$ different parameter values in the range $[-0.013, -0.2] \cup [0.3, 1]$ were used. Depending on the value of θ , the Markov-chain variation parameter r ranged between 3.6% (large $|\theta|$, *i.e.*, $\theta = -0.2$ and $\theta = 1$) and 0.018% (smallest $|\theta|$, *i.e.*, $\theta = -0.013$ here).

We first study the distribution $P(H, t)$ computed with the importance sampling algorithm explained above for the short time $t = 1/16$. The results are shown in fig. 1 for different lengths $L = 64, 128$ and 256 and we compare the numerical results with the analytical result given in eq. (2). The agreement for negative H is very accurate for all lengths, over 800 decades in probability. For positive H slight deviations are visible, but they become smaller with increasing the length L of the polymer, indicating a convergence to the analytical results as well. The behaviour of the extreme left and right tails is also shown in fig. 3.

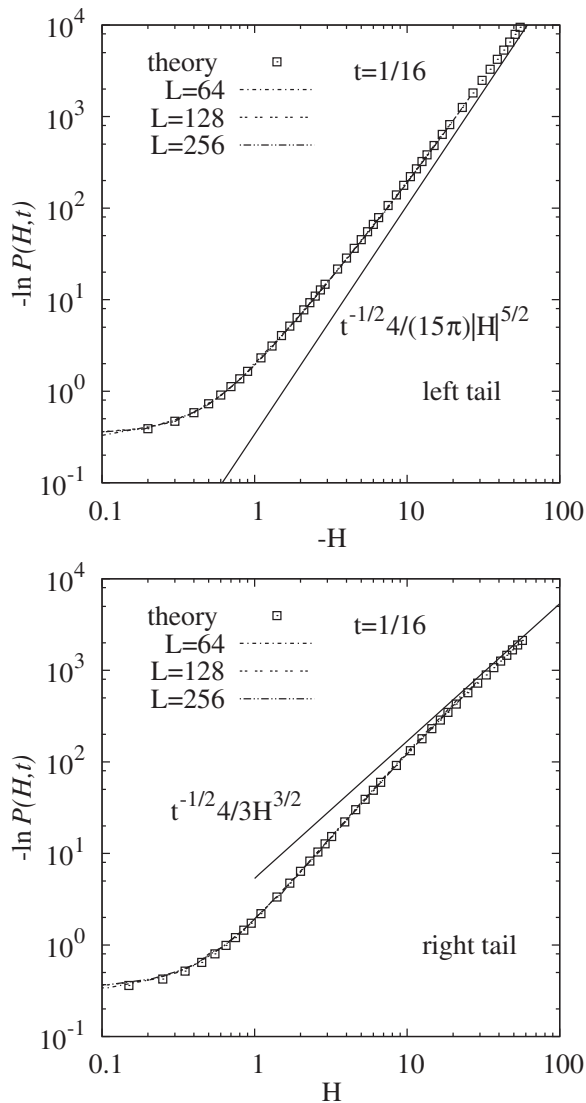


Fig. 3: Top: blowup of the left tail of the data shown in fig. 1 compared to the analytical prediction given in the first line of eq. (3). Bottom: blowup of the right tail data shown in fig. 1 compared to the analytical prediction given in the third line of eq. (3).

In fig. 4 the distributions $P(H, t)$ are shown for increasing times $t = 1/16$, $t = 1/4$ and $t = 32$ together with the Tracy-Widom and the short-time distributions. Here we want to compare only the distribution shapes and, therefore, we have normalised all the curves to have mean zero and unit variance. Regarding the relatively large time $t = 32$ in the typical region (fig. 4, inset) the numerical data clearly differ from the short-time predictions and are closer to the Tracy-Widom distribution. The right tail is very well described by the behaviour predicted in eq. (4) and eq. (5) but the far left tail clearly differs from the Tracy-Widom tail.

To investigate further the long-time behaviour in the negative H tail, we compare the result for $t = 32$ directly with the analytic result in eq. (6). For better visibility,

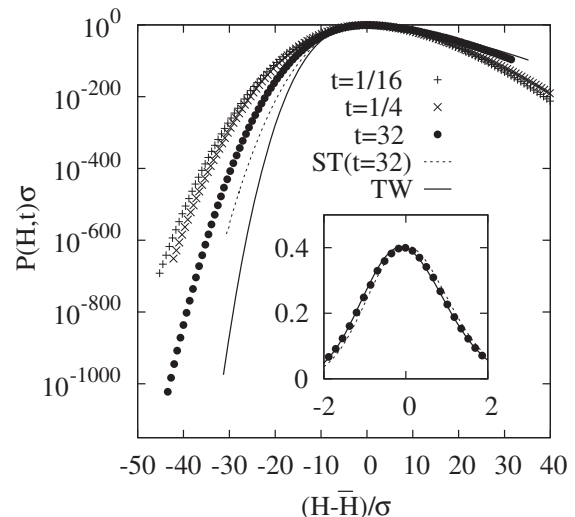


Fig. 4: Distribution of $P(H, t)$ for short ($t = 1/16$), medium ($t = 1/4$) and longer time ($t = 32$) for the longest length $L = 256$. All data are normalised to mean zero and variance one. The solid line shows the Tracy-Widom distribution, the dashed line the short-time result given in eq. (2) with $t = 32$. The inset magnifies the region of high probability for the $t = 32$ case and the two analytical results.

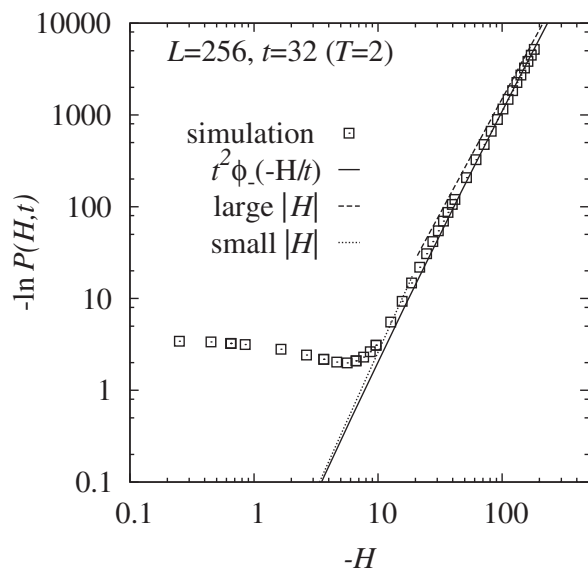


Fig. 5: Logarithm of the left tail of $P(H, t)$ for a longer time ($t = 32$) and for the longest length $L = 256$, shown in double-logarithmic scale. The solid line shows the analytical prediction of eq. (6). The broken line shows the resulting limiting power law: $|H|^3/(12t)$ for very large H , and $\frac{4}{15\pi}|H|^{5/2}/\sqrt{t}$ for moderately large H .

$-\ln(P(H, t))$ is shown in fig. 5 together with the analytic prediction of eq. (6). For the largest values of $-H$ accessible here, a convergence towards the power law $(-H)^{5/2}$ can be observed. Note that the limiting $(-H)^3$ behaviour for small values of $z = H/t$ is not visible here. This is

presumably because this regime is too close to the peak of the distribution. Nevertheless, a small bending is visible in the log-log plot, indicating an increase of the power towards 3 for small values of $-H$.

To summarise, a large-deviation sampling approach has been used to measure the distribution $P(H, t)$ of heights for the KPZ equation with a droplet initial condition. This was achieved using a lattice directed polymer model, whose free energy converges in the high-temperature limit to the height of the continuum KPZ equation. This allowed us to determine numerically the probability distribution of the height over a large range of values, allowing for a precise comparison with the analytical predictions. We find that the agreement with the short-time large-deviation function $\phi_{\text{short}}(H)$ predicted by the theory [18] is spectacular, even very far in the tails. Although we cannot strictly reach the large time limit, our intermediate time results are consistent with both the $|H|^{5/2}$ (negative) and $H^{3/2}$ tails predicted by the theory [30]. Our conclusion is that these far tails are mostly stable in time.

* * *

AKH is grateful to the LPTMS for hosting and financially supporting him for two months during his sabbatical visit July and September 2016. The simulations were mostly performed at the HPC clusters HERO and CARL, both located at the University of Oldenburg (Germany) and funded by the DFG through its Major Research Instrumentation Programme (INST 184/108-1 FUGG and INST 184/157-1 FUGG) and the Ministry of Science and Culture (MWK) of the Lower Saxony State. This research was partially supported by ANR grant ANR-17-CE30-0027-01 RaMaTraF.

REFERENCES

- [1] KARDAR M., PARISI G. and ZHANG Y.-C., *Phys. Rev. Lett.*, **56** (1986) 889.
- [2] HALPIN-HEALY T. and ZHANG Y.-C., *Phys. Rep.*, **254** (1995) 215.
- [3] JOHANSSON K., *Commun. Math. Phys.*, **209** (2000) 437.
- [4] PRÄHOFFER M. and SPOHN H., *Phys. Rev. Lett.*, **84** (2000) 4882.
- [5] PRÄHOFFER M. and SPOHN H., *J. Stat. Phys.*, **108** (2002) 1071.
- [6] CALABRESE P., LE DOUSSAL P. and ROSSO A., *EPL*, **90** (2010) 20002.
- [7] DOTSENKO V., *EPL*, **90** (2010) 20003.
- [8] FERRARI P. L. and SPOHN H., *Commun. Math. Phys.*, **265** (2006) 1.
- [9] DE GIER J. and ESSLER F. H., *Phys. Rev. Lett.*, **107** (2011) 010602.
- [10] KRIECHERBAUER T. and KRUG J., *J. Phys. A*, **43** (2010) 403001.
- [11] SCHUTZ G. M., *Exactly solvable models for many-body systems far from equilibrium*, in *Phase Transitions and Critical Phenomena*, edited by DOMB C. and LEBOWITZ J. L., Vol. **19** (Academic Press, San Diego, Cal., USA) 2001, pp. 1–251.
- [12] TAKEUCHI K. A. and SANO M., *Phys. Rev. Lett.*, **104** (2010) 230601.
- [13] TAKEUCHI K. A., SANO M., SASAMOTO T. and SPOHN H., *Sci. Rep.*, **1** (2011) 34.
- [14] MIETTINEN L., MYLLYS M., MERIKOSKI J. and TIMONEN J., *Eur. Phys. J. B*, **46** (2005) 55.
- [15] HUSE D. A., HENLEY C. L. and FISHER D. S., *Phys. Rev. Lett.*, **55** (1985) 2924.
- [16] KRUG J., *Adv. Phys.*, **46** (1997) 139.
- [17] CORWIN I., *Random Matrices*, **1** (2012) 1130001.
- [18] LE DOUSSAL P., MAJUMDAR S. N., ROSSO A. and SCHEHR G., *Phys. Rev. Lett.*, **117** (2016) 070403.
- [19] SASAMOTO T. and SPOHN H., *Phys. Rev. Lett.*, **104** (2010) 230602.
- [20] AMIR G., CORWIN I. and QUASTEL J., *Commun. Pure Appl. Math.*, **64** (2011) 466.
- [21] TRACY C. A. and WIDOM H., *Commun. Math. Phys.*, **159** (1994) 151.
- [22] NICKELSEN D. and TOUCHETTE H., preprint, arXiv:1803.05708 (2018).
- [23] WIO H., DEZA R., ESCUDERO C. and REVELLI J., *Pap. Phys.*, **5** (2014).
- [24] WIO H. S., RODRIGUEZ M. A., GALLEGRO R., REVELLI J. A., ALS A. and DEZA R. R., *Front. Phys.*, **4** (2017) 52.
- [25] KAMENEV A., MEERSON B. and SASOROV P. V., *Phys. Rev. E*, **94** (2016) 032108.
- [26] KOLOKOLOV I. and KORSHUNOV S., *Phys. Rev. B*, **75** (2007) 140201.
- [27] MEERSON B., KATZAV E. and VILENKIN A., *Phys. Rev. Lett.*, **116** (2016) 070601.
- [28] KRAJENBRINK A. and LE DOUSSAL P., *Phys. Rev. E*, **96** (2017) 020102.
- [29] LE DOUSSAL P., MAJUMDAR S. N. and SCHEHR G., *EPL*, **113** (2016) 60004.
- [30] SASOROV P., MEERSON B. and PROLHAC S., *J. Stat. Mech.* (2017) 063203.
- [31] CORWIN I., GHOSAL P., KRAJENBRINK A., DOUSSAL P. L. and TSAI L., preprint, arXiv:1803.05887 (2018).
- [32] BUSTINGORRY S., LE DOUSSAL P. and ROSSO A., *Phys. Rev. B*, **82** (2010) 140201.
- [33] HARTMANN A. K., *Phys. Rev. E*, **65** (2002) 056102.
- [34] HARTMANN A. K., *Eur. Phys. J. B*, **84** (2011) 627.
- [35] ENGEL A., MONASSON R. and HARTMANN A. K., *J. Stat. Phys.*, **117** (2004) 387.
- [36] HARTMANN A. K., *Phys. Rev. Lett.*, **94** (2005) 050601.
- [37] MONTHUS C. and GAREL T., *Phys. Rev. E*, **74** (2006) 051109.
- [38] WOLFSHEIMER S. and HARTMANN A. K., *Phys. Rev. E*, **82** (2010) 021902.
- [39] DRISCOLL T. A. and MAKI K. L., *SIAM Rev.*, **49** (2007) 673.
- [40] SAITO N., IBA Y. and HUKUSHIMA K., *Phys. Rev. E*, **82** (2010) 031142.
- [41] HARTMANN A. K., MAJUMDAR S. N. and ROSSO A., *Phys. Rev. E*, **88** (2013) 022119.
- [42] HARTMANN A. K., *Phys. Rev. E*, **89** (2014) 052103.

- [43] CLAUSSEN G., HARTMANN A. K. and MAJUMDAR S. N., *Phys. Rev. E*, **91** (2015) 052104.
- [44] DEWENTER T., CLAUSSEN G., HARTMANN A. K. and MAJUMDAR S. N., *Phys. Rev. E*, **94** (2016) 052120.
- [45] NEWMAN M. E. J. and BARKEMA G. T., *Monte Carlo Methods in Statistical Physics* (Clarendon Press, Oxford) 1999.
- [46] LANDAU D. P. and BINDER K., *Monte Carlo Simulations in Statistical Physics* (Cambridge University Press, Cambridge) 2000.
- [47] METROPOLIS N., ROSENBLUTH A. W., ROSENBLUTH M. N., TELLER A. and TELLER E., *J. Chem. Phys.*, **21** (1953) 1087.
- [48] HUKUSHIMA K. and NEMOTO K., *J. Phys. Soc. Jpn.*, **65** (1996) 1604.
- [49] HARTMANN A. K., *Sequence alignments*, in *New Optimization Algorithms in Physics*, edited by HARTMANN A. K. and RIEGER H. (Wiley-VCH, Weinheim) 2004, p. 253.
- [50] HARTMANN A. K., *Big Practical Guide to Computer Simulations* (World Scientific, Singapore) 2015.